Korean J. Chem. Eng., 34(5), 1504-1508 (2017)
DOI: 10.1007/s11814-017-0043-z

pISSN: 0256-1115
eISSN: 1975-7220

Highly stable inverted organic photovoltaic cells with a V_2O_5 hole transport layer

Muhammad Zafar*, Ju-Young Yun, and Do-Heyoung Kim*,†**

*School of Chemical Engineering, Chonnam National University, 300 Youngbong-dong, Gwangju 61186, Korea
**Center for Vacuum, Korea Research Institute of Standards and Science, 267 Gajeong-ro, Daejeon 34113, Korea
(*Received 26 January 2017 • accepted 14 February 2017*)

Abstract−The stability of the hole transport layer (HTL) in inverted organic photovoltaic cells is of great interest because the conventional HTL material, PEDOT:PSS, shows limited stability. In this work, solution processed vanadium pentoxide (V_2O_5) was adopted as the HTL, and the effect of annealing on the properties of the HTL was investigated. The inverted organic photovoltaic cell fabricated with V_2O_5 and annealed for 5 min at 165 °C showed the highest power conversion efficiency (PCE) of 3.92%, which is an enhancement of 16% relative to the cell with PEDOT : PSS (PCE=3.36%). The cell with V_2O_5 was also found to be more stable than the PEDOT : PSS cell, in which a 51% decrease in PCE was observed after 96 h. In contrast, over the same interval, the V_2O_5 device maintained a PCE 85% of the original value.

Keywords: Hole Transport Layer, Spin Coating, Inverted Organic Photovoltaic Cell, Vanadium Pentoxide

INTRODUCTION

Solar cells are a clean energy alternative that can convert sunlight directly to electricity, and are currently attracting attention [1-3]. Among various types of solar cells, organic photovoltaic cells (OPVs) are of great interest due to their low production cost, light weight, and potential for flexible device fabrication. Recently, OPVs with a conventional device structure have been reported to achieve power conversion efficiencies (PCE) up to 6% [4]. However, one of the major drawbacks of conventional OPVs is their poor stability under ambient air conditions, under which OPVs can only perform for few days. To resolve the performance and stability issues of OPVs, inverted structure OPVs has been proposed. The conventional OPV device structure is composed of an anode/hole transport layer/active material/electron transport layer/cathode structure, whereas in inverted OPVs this structure is reversed. n-type semiconducting metal oxides such as ZnO or TiO_2 deposited on fluorine-doped tin oxide (FTO) electrodes can act as an electron transport layer (ETL) for accepting electrons. The use of such metal oxides can dramatically improve the stability of inverted OPVs (IOPVs), and reduce the recombination rate at the interface [2,5].

A typical OPV consists of a bulk hetero-junction (BHJ) structure, in which the most commonly used hole transport layer (HTL) material is poly(4-styrene sulfonate)-doped poly(3,4 ethylenedioxythiophene (PEDOT : PSS). However, PEDOT : PSS has limited stability, and thus it has been replaced by transition metal oxides (TMO), which behave like p-type semiconducting materials. It has been proven that several TMOs show a high affinity towards hole extraction in light emitting diodes (LEDs) [6]. Recently, TMO thin films such as NiO, VO_x, MO_x, and WO_x were inserted as HTLs in OPVs [7-13]. These TMOs showed favorable optical and electronic properties such as high optical transmittance and low barrier height at the interface with the photoactive layer due to their high work functions. Furthermore, their broad technological compatibility with optoelectronics as well as a tendency toward low temperature deposition methods using solution based routes make them an effective alternative. Previous studies mostly used CVD, evaporation, sol-gel, and sputtering techniques under inert conditions for the coating of TMO thin films in OPVs. In contrast to earlier reports, we aimed to obtain V_2O_5 based IOPVs for which all fabrication steps were carried out under ambient air conditions, except for the last top electrode preparation, which was carried out under vacuum, and V_2O_5 at different annealing conditions. The experimental parameters for depositing V_2O_5 films using solution based routes were optimized for obtaining high photovoltaic performance. We report that a PCE of more than 3.9% can be achieved by using the solution based deposition of V_2O_5 films, while the stability of the V_2O_5 based IOPVs is superior to that of devices with PEDOT : PSS.

EXPERIMENTAL

Inverted OPVs were constructed with a cathode/ETL/photoactive/HTL/anode device structure, as shown in Fig. 1. Fig. 2 shows the band gap configurations of the materials used for the device. The holes generated from excitons in the photoactive material (P3HT : PCBM) are collected through the V_2O_5. Spin coated V_2O_5 films were applied onto the photoactive material and were subsequently annealed. Annealing was under various conditions to investigate its effect on the device performance.

1. Materials

The substrate was FTO on glass (with a sheet resistance ≤15 Ω/square and a transmittance >90%), purchased from the Korea Electronics Training Institute. The P3HT and $PC_{60}BM$ were purchased from Rieke Metals and Nano-C, respectively. In addition, the hole

†To whom correspondence should be addressed.
E-mail: kdhh@chonnam.ac.kr

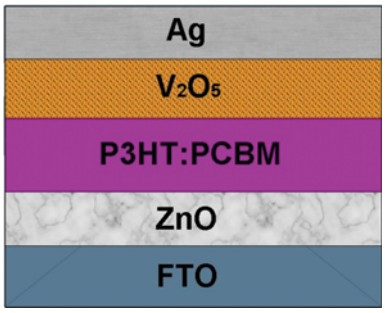

Fig. 1. Schematic structure of V_2O_5-based IOPVs.

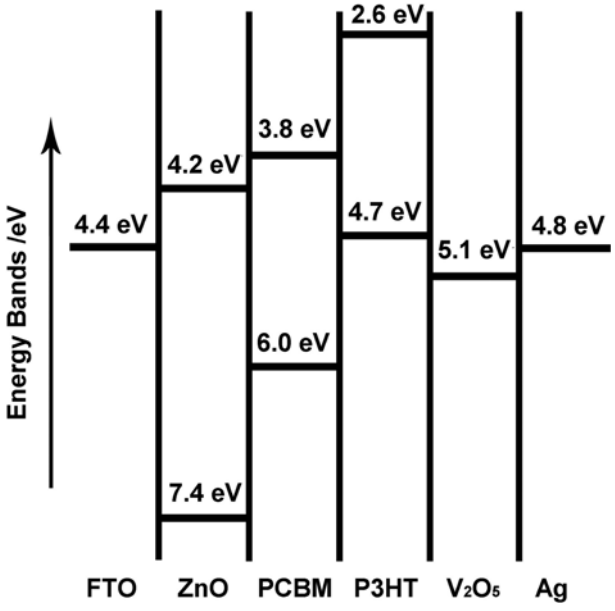

Fig. 2. Energy level distribution diagram of the materials involved in the IOPVs.

transport layer material (PEDOT : PSS) was purchased from Plexcore. All chemicals, including isopropyl alcohol (IPA), chlorobenzene, zinc acetate dihydrate (ZAD), ethanol amine (EA), ethanol, and vanadium oxytriisopropoxide, were purchased from Sigma-Aldrich and were 99% pure.

2. Synthesis of V_2O_5 Films

The V_2O_5 films were formed by the solution process method. The V_2O_5 films were spin-coated from an isopropanol solution of vanadium(V) oxitriisopropoxide with a 1 : 150 volume ratio. The resulting film thickness was 10 nm. The films were subsequently annealed at an optimized temperature of 165 °C at different time intervals (5, 10, 15 mins), and one of the samples was stored at room temperature for 60 min.

3. Fabrication and Characterization of IOPV Devices

FTO-coated glass substrates were cleaned by sonication, first in isopropyl alcohol and then in acetone, for 20 min. The ZnO ETL was prepared with equimolar solutions (0.23 M) of ZAD and EA in ethanol, which were mixed at 80 °C for 24 h. The solution was spin-coated on cleaned FTO substrates that were subsequently heated at 175 °C for 2 h. The resulting film thickness was 25 nm. Then the photoactive layer (P3HT : PCBM) was prepared with a weight ratio of 1 : 0.8 in chlorobenzene that was spin-coated followed by room temperature solvent evaporation for 10 min. Subsequently, the HTL, PEDOT : PSS (1 : 1 vol%), was spin-coated on the surface of the active layer, and then annealed at 165 °C for 5-15 min. Five types of HTL samples were prepared: PEDOT : PSS, V_2O_5 A (stored at room temperature for 60 min), V_2O_5 B (annealed at 165 °C for 5 min), V_2O_5 C (annealed at 165 °C for 10 min) and V_2O_5 D (annealed at 165 °C for 15 min). The Ag electrode was thermally evaporated on top of the HTL through a shadow mask under vacuum. The effective area of the device was 3 mm^2.

The thickness and surface roughness of the films were measured by ellipsometry (Gaertner Scientific) and atomic force microscopy (AFM, Park system), respectively. In addition, the optical transmittance of the samples was measured by UV-visible spectrophotometry (VARIAN). The photovoltaic performance of the samples was evaluated using a solar simulator (Keithley 2400) under 100 mW/cm^2 AM 1.5G. Finally, the external quantum efficiency (EQE) was obtained using a 200 W Xe lamp with a grating monochromator, where light intensity was calibrated using a standard silicon solar cell as a reference (Mc-science).

RESULTS AND DISCUSSION

The V_2O_5 films were fabricated by using the solution processing method, and the thickness was optimized to 10 nm by spin coating. Thin films are preferred for solar cell applications since they reduce the interface between the photoactive materials and HTL, thereby enhancing the hole collection capability. However, in our work, the IOPV device with a HTL thickness greater than 10 nm showed poor photovoltaic performance due to increased series resistance at the interphase and longer hole extraction times [14]. In addition, we used room temperature storage conditions and annealing at different time intervals of 5, 10, 15 min at a temperature

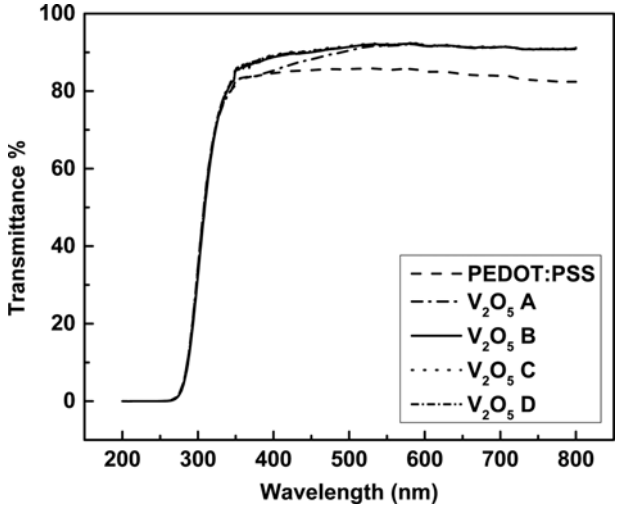

Fig. 3. Transmittance spectra of PEDOT : PSS, V_2O_5 A film stored at room temp. for 60 mins, V_2O_5 B film annealed at 165 °C for 5 mins, V_2O_5 C film annealed at 165 °C for 10 mins and V_2O_5 D film annealed at 165 °C for 15 mins.

Table 1. Photovoltaic properties of the IOPVs with different HTLs

Devices	V_{OC} (V)	J_{SC} (mA/cm^2)	FF (%)	R_{shunt} (Ω)	R_{series} (Ω)	Best PCE (%)	Average PCE (%)
PEDOT : PSS	0.61	10.31	53.13	11296	312	3.36	3.14±0.22
V_2O_5 A	0.60	9.69	58.46	12858	326	3.42	3.31±0.11
V_2O_5 B	0.61	10.68	59.83	15868	298	3.92	3.83±0.09
V_2O_5 C	0.60	9.44	53.30	10476	397	3.01	2.82±0.19
V_2O_5 D	0.60	9.04	52.42	9258	368	2.85	2.67±0.18

V_2O_5 A film stored at room temp. for 60 mins, V_2O_5 B film annealed at 165 °C for 5 mins, V_2O_5 C film annealed at 165 °C for 10 mins and V_2O_5 D film annealed at 165 °C for 15 mins

of 165 °C, which caused slight changes in the composition of the films, as evidenced by the XPS results discussed later. We restricted the annealing to 165 °C because higher temperatures resulted in the thermal degradation of the photo-active material, thereby lowering the device performance [15]. Generally, in UV-spectroscopic analyses, lower transmittance spectra indicate the formation of a thicker film. Fig. 3 shows the transmittance spectra of the PEDOT : PSS and the V_2O_5 films. It is evident that the PEDOT : PSS exhibits low transmittance relative to the V_2O_5 films. The transmittance of the V_2O_5 films increased with increasing annealing time and temperature, which is indicative of the conversion of the precursor to thin V_2O_5 films by removal of the solvent [16].

The photovoltaic performance parameters of the IOPVs with PEDOT : PSS and V_2O_5 films (the latter with different annealing temperatures and times) are summarized in Table 1. The corresponding J-V curves are shown in Fig. 4. The reference device, i.e., the one with the PEDOT : PSS film, shows an open circuit voltage (V_{oc}) of 0.61 V, short circuit current density (J_{sc}) of 10.31 mA/cm^2, fill-factor (FF) of 53.13, and PCE of 3.36%. In comparison to the reference device, the performance of the device V_2O_5 A, stored at room temperature for 60 mins, showed elevated performance parameters but was nevertheless inferior to device V_2O_5 B. The performance of device V_2O_5 B was considerably improved because of the annealing at 165 °C for 5 mins applied to the HTL. Also, the PCEs of the devices decreased when the annealing time was increased to 10 and 15 mins. This was due to the prolonged annealing of the photoactive layer, which degrades when annealed for longer times, together with the HTL. The highest PCE was achieved from device V_2O_5 B, which exhibited a V_{oc} of 0.61 V, J_{sc} of 10.68 mA/cm^2, FF of 59.83, and PCE of 3.92%. In the case of the IOPVs annealed at 165 °C for 10 and 15 mins (V_2O_5 C and V_2O_5 D), the PCE decreased significantly. As shown in Table 1, the shunt resistance (R_{sh}) decreased while the series resistance (R_s) increased with the increase in annealing time in V_2O_5 C and V_2O_5 D, when compared with device V_2O_5 B. It is well known that the R_s value is related to the contact resistance at the interfaces and the bulk resistance of all interfacial layers in the entire IOPV. In addition, R_{sh} reveals the loss of charge carriers due to current leakage pathways and charge recombination in the bulk or at the interface [17,18]. Furthermore, the V_{oc} values of all the devices were almost identical as there were no changes in the properties of the ETL. However, the J_{sc} and FF improved in the device with the optimized HTL, i.e., device V_2O_5 B.

One of the advantages of spin coating is its ability to produce

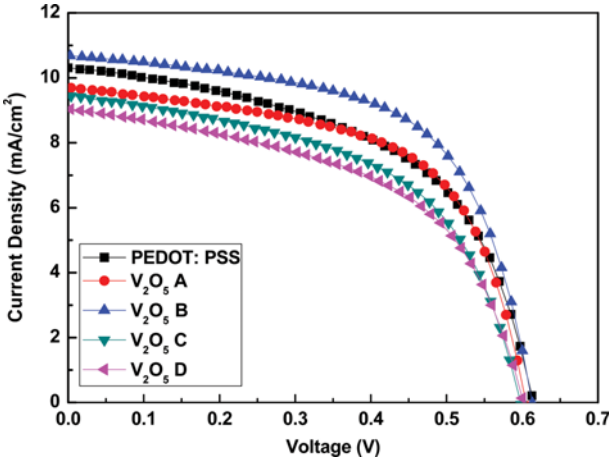

Fig. 4. J-V characteristics of IOPVs with different HTLs. V_2O_5 A film stored at room temp. for 60 mins, V_2O_5 B film annealed at 165 °C for 5 mins, V_2O_5 C film annealed at 165 °C for 10 mins and V_2O_5 D film annealed at 165 °C for 15 mins.

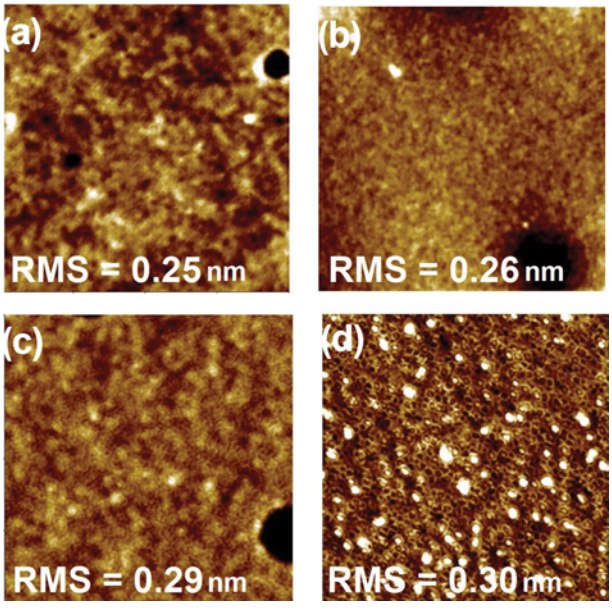

Fig. 5. AFM images of the surface of (a) V_2O_5 A film, stored at room temp. for 60 mins. (b) V_2O_5 B film, annealed at 165 °C for 5 mins. (c) V_2O_5 C film, annealed at 165 °C for 10 mins. (d) V_2O_5 D film, annealed at 165 °C for 15 mins.

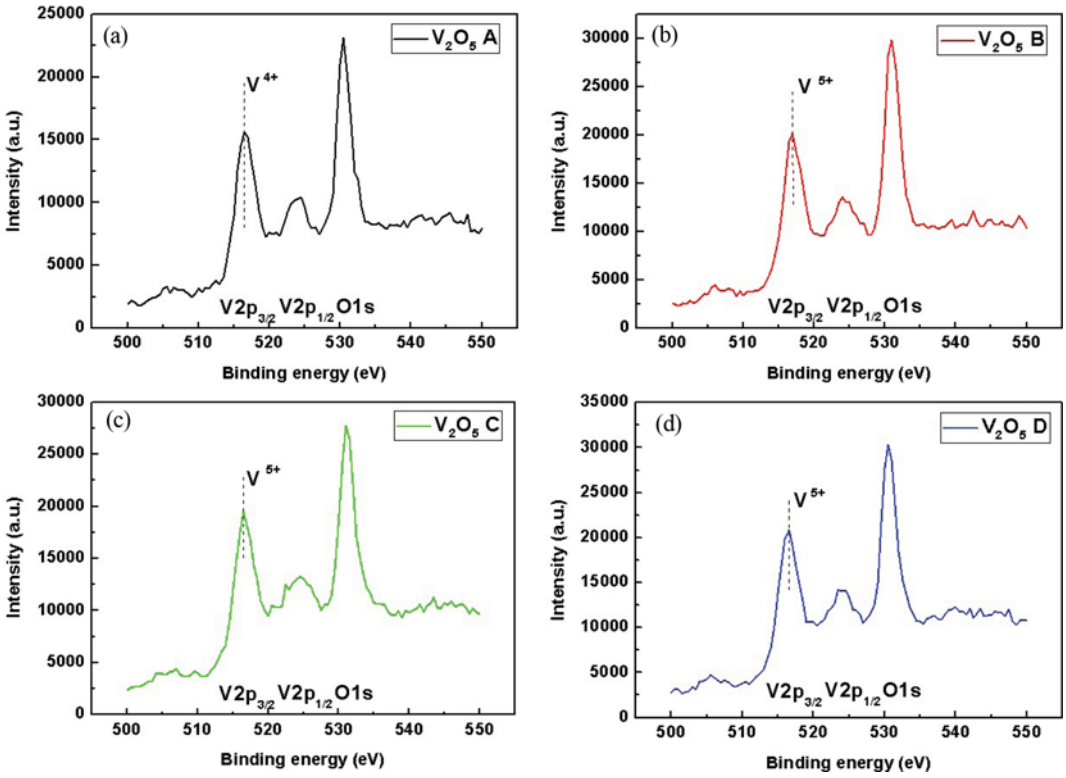

Fig. 6. XPS spectra of (a) V_2O_5 A film, stored at room temp. for 60 mins. (b) V_2O_5 B film, annealed at 165 °C for 5 mins. (c) V_2O_5 C film, annealed at 165 °C for 10 mins. (d) V_2O_5 D film, annealed at 165 °C for 15 mins.

uniform films [2,5]. Fig. 5 shows AFM images of the V_2O_5 films which indicate that, as the annealing temperature and time were increased, the RMS value increased slightly from 0.26 nm to 0.30 nm. This indicates a potential risk for the formation of surface defects between the active layer and HTL as the annealing time is increased. These defects introduce current leakages at the interface and affect the R_s values, as reflected in our results shown in Table 1 [19].

Next, to confirm the successful formation of V_2O_5 and possibility of selective hole transport and collection, compositional analysis was performed through XPS measurement as shown in Fig. 6. The main peak of sample V_2O_5 A, $V2p_{3/2}$, by spin coating is at 516.4 eV, which corresponds to the binding energy of VO_2 and indicates that the oxidation state of vanadium was V^{4+} [14,20]. This result suggests a reason for the low photovoltaic performance of the device V_2O_5 A, in that the potential for the creation of oxygen vacancies will lead to poor hole extraction at the interface. In the case of sample V_2O_5 B, the corresponding $V2p_{3/2}$ peak was at 516.9 eV, which matches the binding energy of V_2O_5 and confirms the complete oxidation of the precursor to V^{5+}. This explains the considerably higher device performance of V_2O_5 B relative to the other fabricated devices. As for samples V_2O_5 C and V_2O_5 D, the corresponding $V2p_{3/2}$ peaks were at 516.5 and 516.6 eV, respectively, which is in close agreement with the binding energy of V_2O_5. This suggests that prolonged annealing stabilizes the precursor at the V_2O_5 state. However, increased annealing times resulted in higher carbon contents in the samples. Notably, the carbon content in V_2O_5 A, V_2O_5 B, V_2O_5 C, and V_2O_5 D was 6.7, 7.7, 8.7, and 9.7%, respectively. The increased carbon content in samples V_2O_5 C and V_2O_5 D led to poor photovoltaic performance [14]. Collectively, these results indicate that the chemical binding state of the spin coated V_2O_5 HTL is close to that of sputtered V_2O_5 films [21].

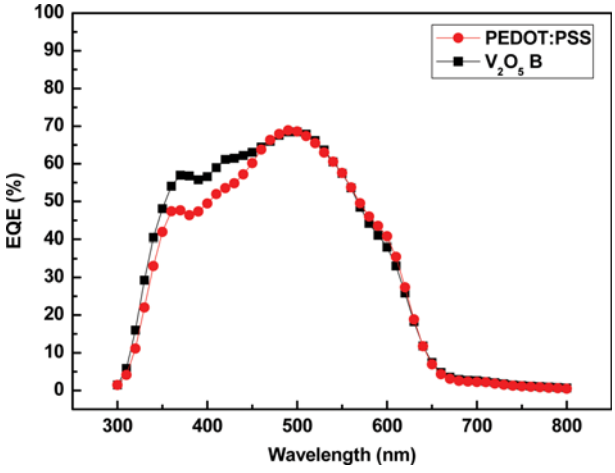

Fig. 7. EQE spectra of IOPVs with PEDOT : PSS and V_2O_5 B film annealed at 165 °C for 5 mins.

The external quantum efficiency (EQE) of selected devices is shown in Fig. 7. I EQE of device V_2O_5 B is slightly better compared to the device with the PEDOT : PSS HTL. And it is increased significantly from 300 to 450 nm compared to device with PEDOT : PSS HTL. The improvement in EQE suggests a higher minority carrier lifetime, which results in an overall increase of the J_{sc} and

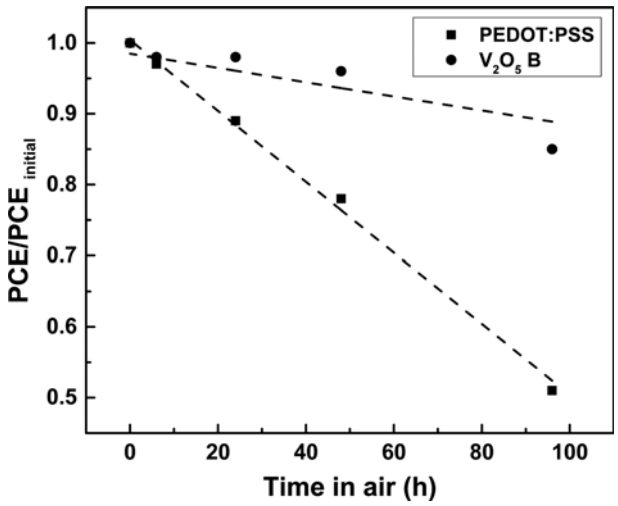

Fig. 8. Stability study of the power conversion efficiency of IOPVs with a PEDOT : PSS and a solution processed V_2O_5 B film annealed at 165 °C for 5 mins. The samples were kept in ambient air.

PCE [22].

The environmental stability of the devices fabricated with V_2O_5 B and PEDOT : PSS HTL was investigated under exposure to ambient air conditions. The temperature and humidity level of the laboratory environment were 25 °C and 50%, respectively. The PCEs of the devices were measured at different time intervals. According to the results depicted in Fig. 8, the solar cell PCE decreased rapidly in the device with the PEDOT : PSS layer compared to the device with the V_2O_5 layer. A decrease of 51% was observed in the PEDOT : PSS device after 96 h, whereas the PCE of the V_2O_5 B device was maintained at 85%. Therefore, the V_2O_5 film behaves as both an effective hole transport layer and a layer protecting the photoactive region from degradation. The accelerated degradation of the PEDOT : PSS based device was apparently due to the acidic nature of its molecules, and to its tendency to absorb moisture from the surrounding environment [20,23]. Furthermore, V_2O_5 thin films are more hydrophobic than PEDOT : PSS, which facilitates better device performance.

CONCLUSION

IOPVs were fabricated with solution processed V_2O_5 hole transport layers and ZnO electron transport layers synthesized using sol-gel methods. The inverted structure took the form FTO/ZnO/P3HT : PCBM/V_2O_5/Ag. We found the optimal thickness of the ZnO and V_2O_5 layers to be 25 nm and 10 nm, respectively. The highest PCE of 3.92% under AM 1.5 illumination at 1,000 W/m^2 was achieved under the optimized annealing condition of 165 °C for 5 mins. This device also showed high stability under ambient air conditions when compared with the reference PEDOT : PSS device over a time span of 96 h.

ACKNOWLEDGEMENTS

This research was supported by the National Research Foundation of Korea, funded by the Ministry of Education, Science and Technology, Korea (NRF-2015M3A7B4050424). In addition, this research was supported by the Development Program of Measurement Technology for Advanced Ultra-Thin Film Processing in the Korea Research Institute of Standards and Science.

REFERENCES

1. V. B. Chu, S. J. Park, G. Park, H. S. Jeon, Y. J. Hwang and B. K. Min, *Korean J. Chem. Eng.*, **33**, 880 (2016).
2. V. H. T. Pham, N. T. N. Truong, T. K. Trinh, S. H. Lee and C. Park, *Korean J. Chem. Eng.*, **33**, 678 (2016).
3. H. H. Cho, C. H. Cho, H. Kang, H. Yu, J. H. Oh and B. J. Kim, *Korean J. Chem. Eng.*, **32**, 261 (2015).
4. M. D. Irwin, D. B. Buchholz, A. W. Hains, R. P. H. Chang and T. J. Marks, *Proc. Nat. Ac. Sci.*, **105**, 2783 (2008).
5. H. Kim, S. Nam, J. Jeong, S. Lee, J. Seo, H. Han and Y. Kim, *Korean J. Chem. Eng.*, **31**, 1095 (2014).
6. H. You, Y. Dai, Z. Zhang and D. Ma, *Appl. Phys.*, **101**, 026105 (2007).
7. G. Li, C. W. Chu, V. Shrotriya, J. Huang and Y. Yang, *Appl. Phys. Lett.*, **88**, 253503 (2006).
8. C. Tao, S. Ruan, X. Zhang, G. Xie, L. Shen, X. Kong, W. Dong, C. Liu and W. Chen, *Appl. Phys. Lett.*, **93**, 193307 (2008).
9. A. K. K. Kyaw, X. W. Sun, C. Y. Jiang, G. Q. Lo, D. W. Zhao and D. L. Kwong, *Appl. Phys. Lett.*, **93**, 221107 (2008).
10. D. W. Zhao, P. Liu, X. W. Sun, S. T. Tan, L. Ke and A. K. K. Kyaw, *Appl. Phys. Lett.*, **92**, 173303 (2008).
11. H. H. Liao, L. M. Chen, Z. Xu, G. Li and Y. Yang, *Appl. Phys. Lett.*, **92**, 173303 (2008).
12. K. Takanezawa, K. Tajima and K. Hashimoto, *Appl. Phys. Lett.*, **93**, 063308 (2008).
13. B. Y. Yu, A. Tsai, S. P. Tsai, K. T. Wong, Y. Yang, C. W. Chu1 and J. J. Shyue, *Nanotechnol.*, **19**, 255202 (2008).
14. K. Zilberberg, S. Trost, J. Meyer, A. Kahn, A. Behrendt, D. L. Hecht, R. Frahm and T. Riedl, *Adv. Funct. Mater.*, **21**, 4776 (2011).
15. Y. Kim, A. M. Ballantyne, J. Nelson and D. D. C. Bradley, *Organic Electronics*, **10**, 205 (2009).
16. J. S. Huang, C. Y. Chou, M. Y. Liu, K. H. Tsai, W. H. Lin and C. F. Lin, *Organic Electronics*, **10**, 1060 (2009).
17. M. Zafar, J. Y. Yun and D. H. Kim, *Appl. Surface Sci.*, **398**, 9 (2017).
18. H. S. Cho, N. Shin, K. Kim, B. Kim and D. H. Kim, *Synthetic Metals*, **207**, 31 (2015).
19. K. Zilberberg, S. Trost, H. Schmidt and T. Riedl, *Adv. Energy Mater.*, **1**, 377 (2011).
20. G. T. Escobar, J. Pampel, J. M. Caicedo and M. L. Cantú, *Energy Environ. Sci.*, **6**, 3088 (2013).
21. S. P. Cho, J. S. Yeo, D. Y. Kim, S. Na and S. S. Kim, *Sol. Energy Mater. Sol. Cells*, **132**, 196 (2015).
22. J. Pann, P. Li, L. Cai, Y. Hu and Y. Zhang, *Sol. Energy Mater. Sol. Cells*, **144**, 616 (2016).
23. E. A. A. Arbab and G. T. Mola, *Appl. Phys. A*, **122**, 405 (2016).